

Received: 2020.03.11

Accepted: 2020.04.06

Published: 2020.06.01

Anti-Alzheimer's Disease Molecular Mechanism of *Acori Tatarinowii Rhizoma* Based on Network Pharmacology

Authors' Contribution:
Study Design A
Data Collection B
Statistical Analysis C
Data Interpretation D
Manuscript Preparation E
Literature Search F
Funds Collection G

AE 1 **Yujia Zhang**
B 1 **Yangsheng Wu**
D 1 **Yunbo Fu**
B 1 **Luning Lin**
F 1 **Yiyu Lin**
F 1 **Yehui Zhang**
AC 1 **Liting Ji**
G 2 **Changyu Li**

1 College of Pharmaceutical Sciences, Zhejiang Chinese Medical University, Hangzhou, Zhejiang, P.R. China

2 Department of Chinese Pharmacy, School of Science, Zhejiang Chinese Medical University, Hangzhou, Zhejiang, P.R. China

Corresponding Authors:

Changyu Li, e-mail: lcyzcmu@sina.com, Liting Ji, e-mail: jenny8825@hotmail.com

Source of support:

This work was supported by the National Natural Science Foundation of China [81673839]; the Department of Human Resources and Social Security of Zhejiang Provincial [752213A00404]; the Research Fund project of Zhejiang Chinese Medical University [2018ZG33]; the Science and Technology Innovation Activity Plan and New Talents Plan for College Students in Zhejiang Province [2019R410058]; and the Postdoctoral Science Foundation Funded Project of Zhejiang Province [752213A00404]

Background:

Acori Tatarinowii Rhizoma (ATR), a traditional Chinese herbal medicine, is used to treat Alzheimer's disease (AD), which is a worldwide degenerative brain disease. The aim of this study was to identify the potential mechanism and molecular targets of ATR in AD by using network pharmacology.

Material/Methods:

The potential targets of the active ingredients of ATR were predicted by PharmMapper, and the targets of Alzheimer's disease were searched by DisGeNET. All screened genes were intersected to obtain potential targets for the active ingredients of ATR. The protein-protein interaction network of possible targets was established by STRING, GO Enrichment, and KEGG pathway enrichment analyses using the Annotation of DAVID database. Next, Cytoscape was used to build the "components-targets-pathways" networks. Additionally, a "disease-component-gene-pathways" network was constructed and verified by molecular docking methods. In addition, the active constituents β -asarone and β -caryophyllene were used to detect $A\beta_{1-42}$ -mediated SH-SY5Y cells, and mRNA expression levels of APP, Tau, and core target genes were estimated by qRT-PCR.

Results:

The results showed that the active components of ATR participate in related biological processes such as cancer, inflammation, cellular metabolism, and metabolic pathways and are closely related to the 13 predictive targets: ESR1, PPARG, AR, CASP3, JAK2, MAPK14, MAP2K1, ABL1, PTPN1, NR3C1, MET, INSR, and PRKACA. The ATR active components of β -caryophyllene significantly reduced the mRNA expression levels of APP, TAU, ESR1, PTPN1, and JAK2.

Conclusions:

The targets and mechanism corresponding to the active ingredients of ATR were investigated systematically, and novel ideas and directions were provided to further study the mechanism of ATR in AD.

MeSH Keywords:

Alzheimer Disease • Medicine, Chinese Traditional • Pharmacology • Protein Interaction Maps

Full-text PDF:

<https://www.basic.medscimonit.com/abstract/index/idArt/924203>

 3108

 5

 6

 26



Background

Research shows that more than 24 million people worldwide have dementia, most of whom are considered to have Alzheimer's disease [1]. Alzheimer's disease (AD) is a degenerative brain disease. The main clinical manifestations are memory loss, cognitive dysfunction, and lack of ability to perform activities of daily life. AD involves mental symptoms that can lead to death and greatly reduce quality of life of patients. Moreover, the care and companionship of AD patients places a heavy burden on their families [2]. Thus, there is an urgent need to explore the pathology and pharmacology of AD. Currently, the study of AD pathology mainly focuses on amyloid deposition, tau hyperphosphorylation, and oxidative stress [3]. In recent years, research on AD pathology and pharmacology has continued, but, unfortunately, most of these studies do not benefit clinical treatment. Clinically, treatment of AD still mainly depends on the use of drugs that enhance cholinergic activity of the central nervous system. Drugs used to slow the development of AD symptoms do not suppress the underlying pathology [4]. Currently, no specific anti-AD drugs are available, and safer and more effective drugs are needed for clinical treatment.

In traditional Chinese medicine, AD is defined as brain-spinal-cord nourishment loss and phlegm-blood stasis blocking due to internal damage, and 7 emotions, long-term disease loss, and deficiency of both qi and blood are caused by old age and phlegm and blood stasis in the interior. It belongs to the categories of "dementia", "literary idiot", and "amnesia" with the clinical manifestation of deficiency origin and excess in the superficiality and treatment of eliminating phlegm for resuscitation, benefiting qi for promoting blood circulation and invigorating the heart and kidney. *Acori Tatarinowii Rhizoma* (ATR), the dry rhizome of an *Araceae* family perennial herb, was recorded as

one of the top-grade medicines in "Shennong's Herbal Classic". It has the function of dispelling dampness and appetite, eliminating phlegm for resuscitation, and waking the mind for improving wisdom, and it is used to cure wind-cold-damp arthralgia and cough with dyspnea and complements 5 viscera, opens 9 orifices, improves visual and auditory acuity, and improves pronunciation. Taking it for a long period of time is beneficial to refresh one's mind, relieve forgetfulness, and maintain longevity. Researchers also found that active compounds of ATR can improve the viability of neural progenitor cells [5].

Network pharmacology has an outstanding performance in systems biology and is increasingly used in the field of pharmaceutical research. It is possible to study the potential active components and targets of traditional Chinese medicines at the system level, and to facilitate the interpretation of the network-related relationship between Chinese medicine ingredients and multiple targets with the help of network pharmacology methods [6]. Many scholars have used PharmMapper to obtain the potential targets of drugs [7,8], and this method combines the drug-target network with the biological system network to provide new ideas for drug research and development [9,10].

Therefore, the present study used network pharmacology to explore the role of the active constituents of ATR in determining the action gene of AD and the multidimensional regulation mechanism from the perspective of bioinformatics as a whole. It is of great significance to provide safe and effective support for drug safety in clinical practice. In this study, we evaluated the effect of active compounds from ATR on AD development based on network pharmacology, and we also confirmed the function of 2 active compounds extracted from ATR *in vitro*. Our data provide ideas for further research on the mechanism of ATR in AD treatment (Figure 1).

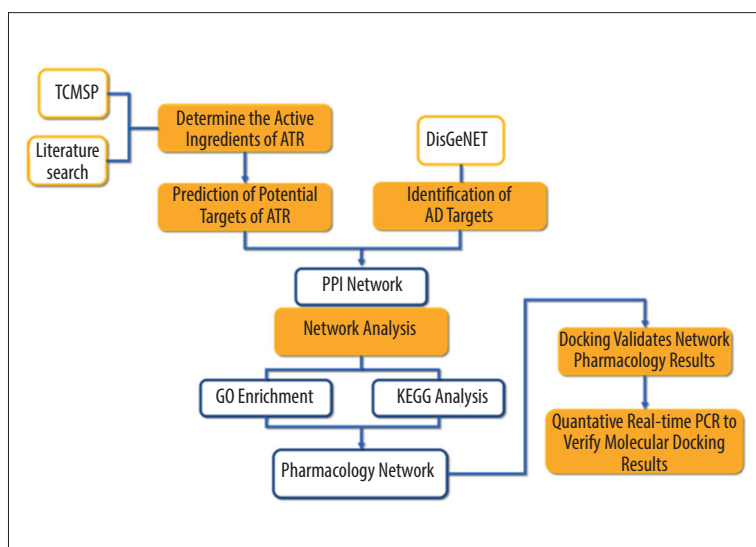


Figure 1. Research Flowchart.

Material and Methods

Data mining

Using the TCMSP (<http://www.tcmspw.com/tcmsp.php>), we searched for the active ingredients of ATR with medicinal (DL) ≥ 0.18 and oral bioavailability (OB) $\geq 30\%$. A search of the TCMSP database identified 61 items. A literature search was performed to determine whether these active ingredients can pass the blood-brain barrier and if they have pharmacological effects, such as sedation, anti-depression, anti-dementia, protection of nerve cells, anti-oxidation, anti-bacterial, and anti-inflammatory [11]. Nine components were identified as research objects.

Prediction of potential targets of ATR

PharmMapper (<http://lilab.ecust.edu.cn/pharmmapper/>) was used, 9 components of the ATR were imported into the database, and small-molecule compounds were used as probes to search for potential drug targets. The values are all default values, and information such as the target name (Target Name), matching value (Fit Score), and function (Function) related to the compound were obtained [12]. We predicted thousands of potential genes through PharmMapper, in descending order of appropriate scores. When one gene symbol for the components of the different subunits was left, we selected the top 10 genes for each active ingredient. Due to the problem of naming irregularities in the searched drug targets, the UniProtKB search function in the UniProt database (<http://www.UniProt.org/>) was used to correct the human-related target codes to their official names [13].

Identification of AD targets

The DisGeNET (<http://www.disgenet.org/>) integrates information on human gene-disease associations (GDAs) and variant-disease associations (VDAs) [14]. A search within DisGeNET for Alzheimer's Disease yielded 1981 potential genes.

PPI network construction and analysis

STRING (<http://string-db.org/>) it is a system that searches for interactions between known proteins and predicts interacting proteins [15]. This interaction involves both direct physical interactions between proteins and the indirect functions of proteins. The potential genes of the ATR effect components were introduced into the STRING online analysis software to obtain the PPI data of the gene-encoding proteins and online mapping, protein interaction network mapping of the genes, and the PPI data of the potential genes from the STRING database were imported into the text format. In Cytoscape software, the protein interaction network was analyzed by NetworkAnalyzer and

evaluated each node with degrees, which represents the number of edges associated with a node in a network.

Annotation analysis of potential target bioinformatics

The obtained gene protein information was subjected to GO enrichment and KEGG analysis using DAVID (<https://david.ncifcrf.gov/>) Bioinformatics Resources 6.8 System and STRING. DAVID now provides a comprehensive set of functional annotation tools for investigators to understand the biological significance behind a large list of genes [16]. With a P value of < 0.05 , we applied a hypergeometric test to identify enriched GO terms.

Pharmacology network of ATR

The potential genes of the 9 components were arranged into component-gene points; the AD-predicted the genes were arranged into a disease-gene, and the gene pathway was made into an Excel spreadsheet with 6 columns. In Cytoscape software, this Excel spreadsheet was imported to construct a component-gene-path network of the gene associated with an AD-related gene. The network contains diseases, components, genes, and action pathways, and 4 types of nodes (nodes); the relationship is represented by edge associations. If the target of the effect component is the same as the gene in the action pathway, they would be connected by an edge to construct a network to study the role of ATR characterized by the multicomponent and multigene-multichannel function in AD treatment.

Docking

SwissDock (<http://www.swissdock.ch/>) is based on the docking software EADock DSS for predicting possible molecular interactions between proteins and small molecules [17,18]. From the PDB database (<http://www.rcsb.org/pdb>), the PDB file that describes the key protein crystal structure in the PPI network was obtained, and the structure of the PDB file and the ligand MOL2 file was imported into SwissDock software for virtual molecular docking analysis of the target protein and active components.

Verification of the molecular docking results

Reagents

Sterilely filtered dimethyl sulfoxide (DMSO) (Sigma-Aldrich) was used to prepare 0.06 mol/L β -asarone (HPLC $\geq 98\%$, source leaf) and 12 mmol/L β -caryophyllene (MACKIN) stock solutions. MEM medium (Gibco), fetal bovine serum (FBS, Gibco), F12 (Gibco) medium, glutamine (Gibco), sodium pyruvate (Gibco), and NEAA (Gibco) were used for cell culture. The amyloid beta fragment 1-42 ($A\beta_{1-42}$, Gil biochemical) was dissolved in DMSO to 10 mmol/L for use. $A\beta_{1-42}$ was diluted to 100 μ mol/L and

Table 1. Primer sequences.

Gene	Primer sequence (5' 3')	Gene	Primer sequence (5' 3')
ESR1-F	ATGGTCAGTGCCCTGTGGATGC	JAK2-F	GTGTGGAGATGTGCCGGTATGAC
ESR1-R	GTCTGCCAGGTGGTTCAGTAAGC	JAK2-R	GATTACGCCGACCAGCACTGTAG
PPKACA-F	GCTACAACAAGGCCGTGGACTG	CASP3-F	AGTGGAGGCCGACTTCTTGT
PPKACA-R	AGGAGGTTCCGCAGCAGGTC	CASP3-R	GGCACAAGCGACTGGATGA
MET-F	TCAGAACGGTTCATGCCGACAAG	PPAGR-F	TCCTCGGTGACTTATCCTGTGGTC
MET-R	CTACATGCTGCACTGCCTGGAC	PPAGR-R	GCGTGGACTCCGTAATGATAGCC
NR3C1-F	CTGCCTGGTGTGCTCTGATGAAG	PDE4D-F	CTCTCGCTTCAGACAGTTGGAAC
NR3C1-R	AATTGTGCTGCTCTTCCACTGCTC	PDE4D-R	AGCAATCAGCGGCAGAATCTTCAG
PTPN1-F	GCTGATACCTGCCTCTTGCTGATG	INSR-F	ATCCGCCGATCTACGCTCTG
PTPN1-R	AGCTGGTCGGCTGTCTGGATC	INSR-R	GCTGCCTTAGGTTCTGGTTGTC
ABL1-F	AGCAACTACATCACGCCAGTCAAC	APP-F	AGGACTGACCACTCGACCAG
ABL1-R	CTCACTCTCACGCCAAGAAGC	APP-R	CGGGGGTCTAGTTCTGCAT
MAP2K1-F	GCCGTGTGGTGTCAAGGTCTC	Tau-F	TGAACCAGGATGGCTGAG
MAP2K1-R	CTGATCTCGCCATCGCTGAGAAC	Tau-R	TTGTCATCGCTTCCAGTCC
MAPK14-F	GGCTCCTGAGATCATGCTGAACTG	GAPDH-F	CAGGAGGCATTGCTGATGAT
MAPK14-R	AGTCAACAGCTCGGCCATTATGC	GAPDH-R	GAAGGCTGGGGCTCATT

incubated at 37°C for 24 h until it formed aggregated diffusible oligomers for the preparation of the AD damage model.

Cell culture and CCK-8 for screening concentration

The human neuroblastoma cell line SH-SY5Y (purchased from the Chinese Academy of Sciences cell bank) was selected and cultured in MEM and F12 complete medium, placed in 5% CO₂, cultured at 37°C in a humid environment, and used for experiments when the cells were 85% confluent. The AD cell injury model was constructed by incubating SH-SY5Y cells in logarithmic growth phase with Aβ₁₋₄₂ diluted to 100 μmol/L in serum-free medium for 48 h. Cell viability was measured using CCK-8 (Cell Counting Kit-8, MedChem Express) and a BioTek Synergy H1 multiplate reader to screen for appropriate concentrations of Aβ₁₋₄₂.

Quantitative real-time PCR to detect gene expression

After 24-h treatment with β-Asarone or β-caryophyllene, RNA extraction from SH-SY5Y cells incubated with Aβ₁₋₄₂ was performed using an extraction kit (TaKaRa). Quantitative real-time PCR (qRT-PCR) was performed with the Bio-Rad CFX96 Real-Time System. A volume of 10 μL containing 0.4 μL of primer (designed by the manufacturer), 1 μL of cDNA, and 5 μL of SYBR Green PCR Master Mix (TaKaRa) was used for qRT-PCR. mRNA levels were normalized to GAPDH mRNA levels, and statistical analysis was performed using the 2^{-ΔΔCt} method. The primer sequences were used for qRT-PCR (Table 1).

Statistics and analysis

In vitro experimental data were statistically analyzed using the IBM SPSS 20.0 software package. One-way ANOVA or nonparametric test was used for comparison between groups. P<0.05 was set as a statistically significant difference. The normal group, the model group, and the drug-administered group were compared to determine whether the differences were statistically significant.

Results

ATR active ingredient information

As show in Table 2, 9 active components were determined to be the most valuable: α-asarone, β-asarone, borneol (-), borneol (+), cis-methyl isoeugenol, trans-methyl isoeugenol, β-caryophyllene (-), β-caryophyllene (+), and α-terpineol.

Screening for the potential genes of ATR to improve AD

According to the structural formulas, 35 related genes were screened by PharmMapper and DisGeNET, which may be potential genes for the treatment of AD using ATR (Table 3).

Pathway enrichment analysis for candidate ATR targets

GO enrichment was divided into 3 parts: biological processes, molecular functions, and cellular components. The 35 genes

Table 2. Chemical information for the constituents of ATR.

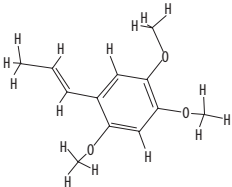
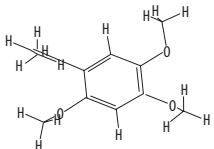
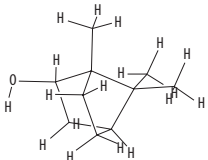
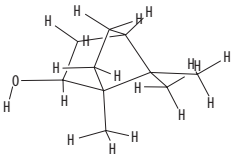
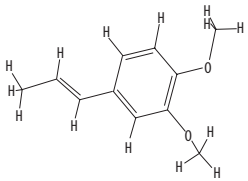
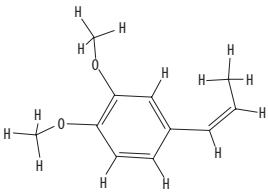
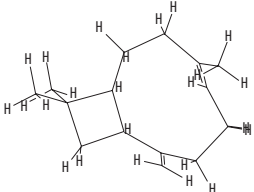
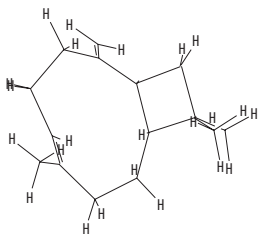
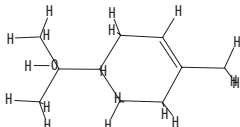
Compounds	MW	Structure	Composition	CAS No.
α -Asarone	208.254		$C_{12}H_{16}O_3$	2883-98-9
β -Asarone	208.254		$C_{12}H_{16}O_3$	5273-86-9
(-)-Borneol	154.249		$C_{10}H_{18}O$	464-45-9
(+)-Borneol	154.249		$C_{10}H_{18}O$	464-43-7
Cis-methyl isoeugenol	178.228		$C_{11}H_{14}O_2$	6380-24-1
Trans-methyl isoeugenol	178.228		$C_{11}H_{14}O_2$	6379-72-2
(-)- β -Caryophyllene	204.351		$C_{15}H_{24}$	87-44-5

Table 2 continued. Chemical information for the constituents of ATR.

Compounds	MW	Structure	Composition	CAS No.
(+)- β -Caryophyllene	204.351		C ₁₅ H ₂₄	87-44-5
α -Terpineol	154.249		C ₁₀ H ₁₈ O	98-55-5

predicted by ATR in AD were enriched by GO enrichment using the DAVID bioinformatics resources. Figure 2 shows the GO analysis results of the potential genes from the ATR calamus effect component. The functional distribution of the potential genes was preliminarily analyzed by GO analysis. In biological processes, we found that biological regulation, organic substance metabolic processes, cellular processes, primary metabolic processes, regulation of biological processes, cellular metabolic processes, and regulation of cellular processes accounted for a large proportion of hits. In molecular function, we found that binding, ion binding, and catalytic activity were closely related. The intracellular, intracellular part and cytoplasm of the cellular components were ranked first and had the largest proportion of hits.

KEGG pathway annotation analysis of STRING showed that the pathway distribution of 35 potential genes, including pathogenesis-related pathways, were mainly involved in pathways in cancer, proteoglycans in cancer, MAPK signaling pathway, metabolic pathways, Ras signaling pathway, and PI3K-Akt signaling pathway. We discovered 103 pathways, including prolactin signaling pathway, bile secretion, and endocrine resistance. Figure 3 shows the top 20 related pathways.

Identification of potential candidate ATR targets

After deleting the isolated pairs of linked nodes, we built a PPI network by Cytoscape, showing 35 proteins evaluated after interaction based on the STRING (version 10.0) database (Figure 4). Finally, a pharmacological network was composed of 35 nodes and 85 edges; the maximum degree of the nodes was 28 and the minimum degree was 1. The connectivity means the higher the node connectivity, the more stable the network is. The average of the nodes in the network was 4.86

and the standard deviation was 0.551. Candidate genes were selected based on the connectivity of each node (set as \geq the mean value+standard deviation). ESR1 (15), PPARG (14), AR (13), CASP3 (12), JAK2 (9), MAPK14 (9), MAP2K1 (9), ABL1 (9), PTPN1 (8), NR3C1 (8), MET (7), INSR (6), and PRKACA (6) were key nodes in maintaining the stability of this pharmacological network and show the potential correlation of AD.

All analytical data were integrated to construct the pharmacology network of ATR

We combined previous data to find the relationships among ATR compositions, potential genes, and selected 20 pathways ($P < 0.05$) by use of a pharmacological network (Figure 5). This network diagram provides basic data for further exploration of mechanism research. Using this network provided a preliminary understanding of the mechanism of ATR in AD. Potential genes of active ingredients interact in various pathways, thereby affecting the occurrence and development of AD.

Docking verification of network pharmacology results

Using the SwissDock software, these 13 core target proteins and corresponding active components were molecularly docked and verified by default parameters to obtain the estimated ΔG values of the docking model. The larger the negative value, the more stable it is. The docking results are shown in Table 4, in which β -caryophyllene (+) has good docking activity with the core target protein.

Cell experiments verify molecular docking results

According to the results of docking, the most popular active ingredients of ATR was β -asarone, and β -caryophyllene had the

Table 3. Potential target information of ATR against AD.

Uniprot ID	Gene	Specie	Protein	Composition
P05413	FABP3	<i>Homo sapiens</i>	Fatty acid binding protein 3	(+)- β -caryophyllene
P03372	ESR1	<i>Homo sapiens</i>	Estrogen receptor 1	(+)- β -caryophyllene
P37231	PPARG	<i>Homo sapiens</i>	Peroxisome proliferator activated receptor gamma	(+)- β -caryophyllene
Q14994	NR1I3	<i>Homo sapiens</i>	Nuclear receptor subfamily 1 group I member 3	(+)- β -caryophyllene
P49638	TTPA	<i>Homo sapiens</i>	alpha tocopherol transfer protein	(-)- β -caryophyllene
P49638	TTPA	<i>Homo sapiens</i>	alpha tocopherol transfer protein	(+)- β -caryophyllene
P09211	GSTP1	<i>Homo sapiens</i>	Glutathione S-transferase pi 1	(+)-Borneol
P10275	AR	<i>Homo sapiens</i>	Androgen receptor	(+)-Borneol
P10275	AR	<i>Homo sapiens</i>	Androgen receptor	(-)- β -caryophyllene
P10275	AR	<i>Homo sapiens</i>	Androgen receptor	(+)- β -caryophyllene
Q02750	MAP2K1	<i>Homo sapiens</i>	Mitogen-activated protein kinase kinase 1	(+)-Borneol
Q02750	MAP2K1	<i>Homo sapiens</i>	Mitogen-activated protein kinase kinase 1	(-)- β -caryophyllene
Q02750	MAP2K1	<i>Homo sapiens</i>	Mitogen-activated protein kinase kinase 1	(+)- β -caryophyllene
P27487	DPP4	<i>Homo sapiens</i>	Dipeptidyl peptidase 4	(-)-Borneol
P27487	DPP4	<i>Homo sapiens</i>	Dipeptidyl peptidase 4	(+)-Borneol
P27487	DPP4	<i>Homo sapiens</i>	Dipeptidyl peptidase 4	(+)- β -caryophyllene
P19793	RXRA	<i>Homo sapiens</i>	Retinoid X receptor alpha	(-)-Borneol
P19793	RXRA	<i>Homo sapiens</i>	Retinoid X receptor alpha	(-)- β -caryophyllene
P19793	RXRA	<i>Homo sapiens</i>	Retinoid X receptor alpha	(+)- β -caryophyllene
P42574	CASP3	<i>Homo sapiens</i>	Caspase 3	(-)-Borneol
P00519	ABL1	<i>Homo sapiens</i>	ABL proto-oncogene 1	(-)-Borneol
P00519	ABL1	<i>Homo sapiens</i>	ABL proto-oncogene 1	(+)-Borneol
P14061	HSD17B1	<i>Homo sapiens</i>	Hydroxysteroid 17-beta dehydrogenase 1	(-)-Borneol
P14061	HSD17B1	<i>Homo sapiens</i>	Hydroxysteroid 17-beta dehydrogenase 1	(+)-Borneol
P14061	HSD17B1	<i>Homo sapiens</i>	Hydroxysteroid 17-beta dehydrogenase 1	(-)- β -caryophyllene
P14061	HSD17B1	<i>Homo sapiens</i>	Hydroxysteroid 17-beta dehydrogenase 1	(+)- β -caryophyllene
P11473	VDR	<i>Homo sapiens</i>	Vitamin D receptor	(-)-Borneol
P11473	VDR	<i>Homo sapiens</i>	Vitamin D receptor	(+)-Borneol
P11473	VDR	<i>Homo sapiens</i>	Vitamin D receptor	(+)- β -caryophyllene
P04278	SHBG	<i>Homo sapiens</i>	Sex hormone binding globulin	(-)-Borneol
P04278	SHBG	<i>Homo sapiens</i>	Sex hormone binding globulin	(+)-Borneol
P04278	SHBG	<i>Homo sapiens</i>	Sex hormone binding globulin	(-)- β -caryophyllene
P08581	MET	<i>Homo sapiens</i>	MET proto-oncogene	α -Terpineol
O60674	JAK2	<i>Homo sapiens</i>	Janus kinase 2	α -Terpineol
Q16539	MAPK14	<i>Homo sapiens</i>	Mitogen-activated protein kinase 14	α -Terpineol

Table 3 continued. Potential target information of ATR against AD.

Uniprot ID	Gene	Specie	Protein	Composition
P04035	HMGCR	<i>Homo sapiens</i>	3-hydroxy-3-methylglutaryl-CoA reductase	Trans-methyl isoeugenol
P02753	RBP4	<i>Homo sapiens</i>	Retinol binding protein 4	Trans-methyl isoeugenol
P02753	RBP4	<i>Homo sapiens</i>	Retinol binding protein 4	(-)- β -caryophyllene
P28845	HSD11B1	<i>Homo sapiens</i>	Hydroxysteroid 11-beta dehydrogenase 1	Trans-methyl isoeugenol
P28845	HSD11B1	<i>Homo sapiens</i>	Hydroxysteroid 11-beta dehydrogenase 1	α -Terpineol
P28845	HSD11B1	<i>Homo sapiens</i>	Hydroxysteroid 11-beta dehydrogenase 1	(-)-Borneol
P28845	HSD11B1	<i>Homo sapiens</i>	Hydroxysteroid 11-beta dehydrogenase 1	(+)-Borneol
P04150	NR3C1	<i>Homo sapiens</i>	Nuclear receptor subfamily 3 group C member 1	Trans-methyl isoeugenol
P04150	NR3C1	<i>Homo sapiens</i>	Nuclear receptor subfamily 3 group C member 1	α -Terpineol
Uniprot ID	Gene	Specie	Protein	Composition
P04150	NR3C1	<i>Homo sapiens</i>	Nuclear receptor subfamily 3 group C member 1	(-)-Borneol
P04150	NR3C1	<i>Homo sapiens</i>	Nuclear receptor subfamily 3 group C member 1	(+)-Borneol
P04150	NR3C1	<i>Homo sapiens</i>	Nuclear receptor subfamily 3 group C member 1	(-)- β -caryophyllene
P04150	NR3C1	<i>Homo sapiens</i>	Nuclear receptor subfamily 3 group C member 1	(+)- β -caryophyllene
P00918	CA2	<i>Homo sapiens</i>	Carbonic anhydrase 2	Trans-methyl isoeugenol
P00918	CA2	<i>Homo sapiens</i>	Carbonic anhydrase 2	α -Terpineol
P00918	CA2	<i>Homo sapiens</i>	Carbonic anhydrase 2	(-)- β -caryophyllene
P00517	PRKACA	<i>Homo sapiens</i>	Protein kinase cAMP-activated catalytic subunit alpha	Trans-methyl isoeugenol
P02766	TTR	<i>Homo sapiens</i>	Transthyretin	Cis-methyl isoeugenol
P02766	TTR	<i>Homo sapiens</i>	Transthyretin	(-)-Borneol
P02766	TTR	<i>Homo sapiens</i>	Transthyretin	(+)-Borneol
P02766	TTR	<i>Homo sapiens</i>	Transthyretin	(-)- β -caryophyllene
P02766	TTR	<i>Homo sapiens</i>	Transthyretin	(+)- β -caryophyllene
P08254	MMP3	<i>Homo sapiens</i>	Matrix metalloproteinase 3	Cis-methyl isoeugenol
P08254	MMP3	<i>Homo sapiens</i>	Matrix metalloproteinase 3	Trans-methyl isoeugenol
P52895	AKR1C2	<i>Homo sapiens</i>	Aldo-keto reductase family 1 member C2	Cis-methyl isoeugenol
P52895	AKR1C2	<i>Homo sapiens</i>	Aldo-keto reductase family 1 member C2	Trans-methyl isoeugenol
P50579	METAP2	<i>Homo sapiens</i>	Methionyl aminopeptidase 2	Cis-methyl isoeugenol
P50579	METAP2	<i>Homo sapiens</i>	Methionyl aminopeptidase 2	Trans-methyl isoeugenol
P50579	METAP2	<i>Homo sapiens</i>	Methionyl aminopeptidase 2	α -Asarone
P06744	GPI	<i>Homo sapiens</i>	Glucose-6-phosphate isomerase	β -Asarone
P06744	GPI	<i>Homo sapiens</i>	Glucose-6-phosphate isomerase	α -Asarone
P06213	INSR	<i>Homo sapiens</i>	Insulin receptor	β -Asarone
P06213	INSR	<i>Homo sapiens</i>	Insulin receptor	Cis-methyl isoeugenol

Table 3 continued. Potential target information of ATR against AD.

Uniprot ID	Gene	Specie	Protein	Composition
P06213	INSR	<i>Homo sapiens</i>	Insulin receptor	α -Terpineol
P06213	INSR	<i>Homo sapiens</i>	Insulin receptor	α -Asarone
P56817	BACE1	<i>Homo sapiens</i>	beta-secretase 1	β -Asarone
P56817	BACE1	<i>Homo sapiens</i>	beta-secretase 1	Trans-methyl isoeugenol
P56817	BACE1	<i>Homo sapiens</i>	beta-secretase 1	α -Terpineol
P56817	BACE1	<i>Homo sapiens</i>	beta-secretase 1	α -Asarone
P18031	PTPN1	<i>Homo sapiens</i>	Protein tyrosine phosphatase non-receptor type 1	β -Asarone
P18031	PTPN1	<i>Homo sapiens</i>	Protein tyrosine phosphatase non-receptor type 1	Cis-methyl isoeugenol
P18031	PTPN1	<i>Homo sapiens</i>	Protein tyrosine phosphatase non-receptor type 1	Trans-methyl isoeugenol
P18031	PTPN1	<i>Homo sapiens</i>	Protein tyrosine phosphatase non-receptor type 1	α -Terpineol
P18031	PTPN1	<i>Homo sapiens</i>	Protein tyrosine phosphatase non-receptor type 1	α -Asarone
P14324	FDPS	<i>Homo sapiens</i>	Farnesyl diphosphate synthase	β -Asarone
P14324	FDPS	<i>Homo sapiens</i>	Farnesyl diphosphate synthase	α -Asarone
P27338	MAOB	<i>Homo sapiens</i>	Monoamine oxidase B	β -Asarone
P27338	MAOB	<i>Homo sapiens</i>	Monoamine oxidase B	Cis-methyl isoeugenol
P27338	MAOB	<i>Homo sapiens</i>	Monoamine oxidase B	Trans-methyl isoeugenol
P27338	MAOB	<i>Homo sapiens</i>	Monoamine oxidase B	α -Asarone
P08473	MME	<i>Homo sapiens</i>	Membrane metalloendopeptidase	β -Asarone
P08473	MME	<i>Homo sapiens</i>	Membrane metalloendopeptidase	Cis-methyl isoeugenol
P08473	MME	<i>Homo sapiens</i>	Membrane metalloendopeptidase	α -Asarone

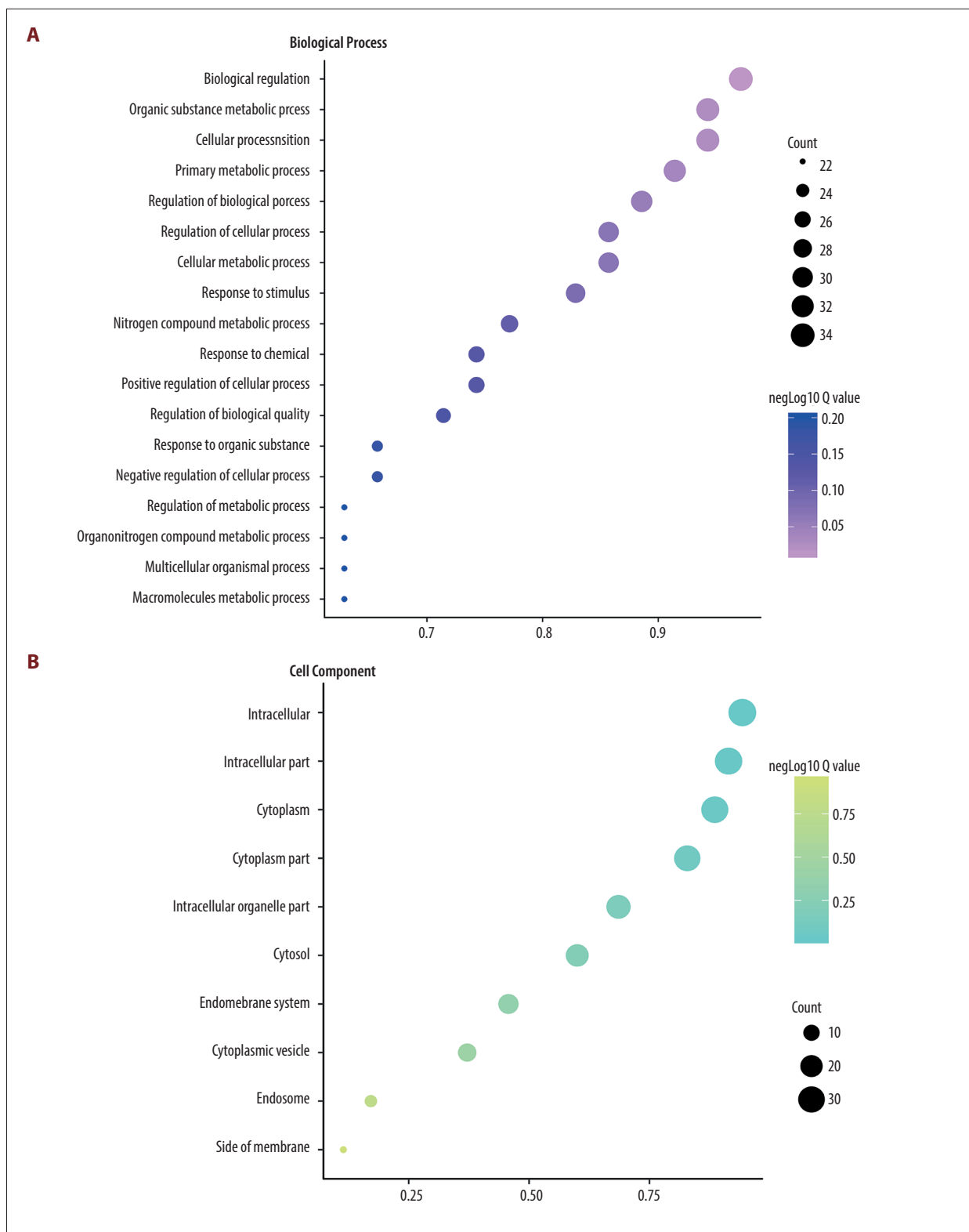
best docking stability; therefore, these active ingredients were selected for further efficacy verification. As shown in Table 5, there were no significant differences between the DMSO group and the normal group; the cell viability of $A\beta_{1-42}$ (50 $\mu\text{mol/L}$ and 100 $\mu\text{mol/L}$) cells was significantly lower than the normal and the DMSO groups. The expression levels of the AD marker genes APP and TAU were detected by qRT-PCR (Figure 6A, 6B). They were significantly upregulated after the modeling, and the mRNA expression level was significantly decreased after incubating with the active ingredient.

According to Figure 6C–6N, compared with the normal group, the mRNA levels of CASP3, ESR1, MET, JAK2, and PTPN1 in the $A\beta_{1-42}$ module were significantly increased, and the mRNA levels of PRKACA, ABL1, and INSR genes were significantly reduced. Compared with the $A\beta_{1-42}$ model, after administration of β -asarone, PPAGR, PRKACA, MET, ABL1, and MAP2K1 mRNA expression levels were significantly upregulated, and ESR1, NR3C1, JAK2, and PTPN1 mRNA expression levels were significantly reduced. Comparison of the β -caryophyllene administration

group with $A\beta_{1-42}$ alone showed that the mRNA expression levels of ESR1, JAK2, and PTPN1 were significantly lower, and the mRNAs of PRKACA, ABL1 and MAP2K1 were significantly higher.

Discussion

In this study, using the TCMS system and a literature research, 9 active ingredients of ATR were screened. As a research object, the possible targets and pathways of the components were analyzed by means of network pharmacology. Along with the outstanding performance of the network pharmacology in systems biology, the network pharmacology-based PharmMapper is increasingly popular in the field of drug research. Saleem et al. found putative targets that potentially interact with 2 new maleates (F9 and CB18) of *Pteris cretica* L. through reverse docking by using the in-silico tools PharmMapper and ReverseScreen3D [19]. Zhang discovered the potential molecular targets of SQW treatment for KYDS through PharmMapper [20]. Therefore, we selected PharmMapper as a



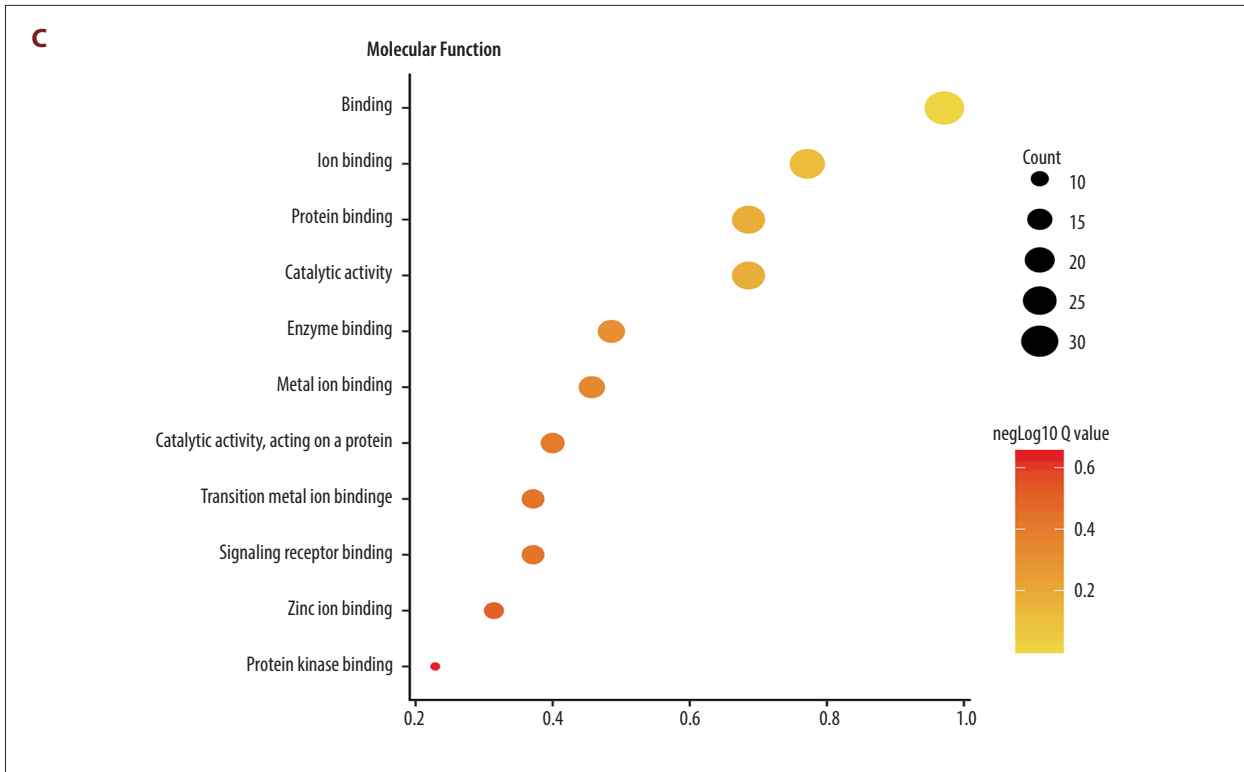


Figure 2. GO enrichment analysis of the potential genes predicted in the PharmMapper database. (A) Biological Process; (B) Cellular Component; (C) Molecular Function.

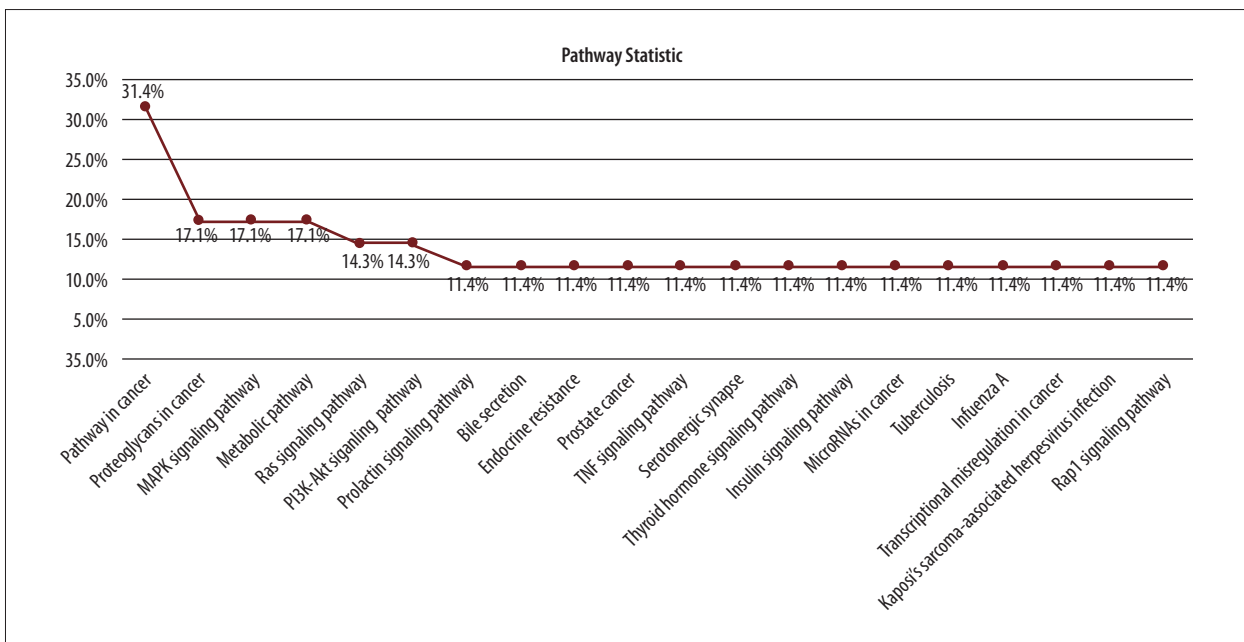


Figure 3. KEGG enrichment pathways of the top 20 potential genes in ATR.

Table 4. Molecular docking results of core targets and active components of ATR.

Gene	Composition	Specie	Protein	PDB ID	Estimated ΔG (kcal/mol)
AR	(+)- β -caryophyllene	<i>Homo sapiens</i>	Androgen receptor	1GS4	-7.96
ESR1	(+)- β -caryophyllene	<i>Homo sapiens</i>	Estrogen receptor 1	ISJO	-7.78
AR	(-)- β -caryophyllene	<i>Homo sapiens</i>	Androgen receptor	1GS4	-7.69
PPARG	(+)- β -caryophyllene	<i>Homo sapiens</i>	Peroxisome proliferator activated receptor gamma	1KNU	-7.37
AR	(+)-Borneol	<i>Homo sapiens</i>	Androgen receptor	1GS4	-7.04
INSR	α -Asarone	<i>Homo sapiens</i>	Insulin receptor	3EKK	-7.01
INSR	β -Asarone	<i>Homo sapiens</i>	Insulin receptor	3EKK	-7.01
NR3C1	Trans-methyl isoeugenol	<i>Homo sapiens</i>	Nuclear receptor subfamily 3 group C member 1	3E7C	-6.95
NR3C1	α -Terpineol	<i>Homo sapiens</i>	Nuclear receptor subfamily 3 group C member 1	3E7C	-6.87
NR3C1	(-)- β -caryophyllene	<i>Homo sapiens</i>	Nuclear receptor subfamily 3 group C member 1	3E7C	-6.87
NR3C1	(+)- β -caryophyllene	<i>Homo sapiens</i>	Nuclear receptor subfamily 3 group C member 1	3E7C	-6.84
INSR	α -Terpineol	<i>Homo sapiens</i>	Insulin receptor	3EKK	-6.81
JAK2	α -Terpineol	<i>Homo sapiens</i>	Janus kinase 2	3E64	-6.81
PTPN1	Cis-methyl isoeugenol	<i>Homo sapiens</i>	Protein tyrosine phosphatase non-receptor type 1	1ONY	-6.72
PRKACA	Trans-methyl isoeugenol	<i>Homo sapiens</i>	Protein kinase cAMP-activated catalytic subunit alpha	1Q8T	-6.64
INSR	Cis-methyl isoeugenol	<i>Homo sapiens</i>	Insulin receptor	3EKK	-6.64
PTPN1	α -Asarone	<i>Homo sapiens</i>	Protein tyrosine phosphatase non-receptor type 1	1ONY	-6.62
PTPN1	Trans-methyl isoeugenol	<i>Homo sapiens</i>	Protein tyrosine phosphatase non-receptor type 1	1ONY	-6.55
PTPN1	β -Asarone	<i>Homo sapiens</i>	Protein tyrosine phosphatase non-receptor type 1	1ONY	-6.55
MET	α -Terpineol	<i>Homo sapiens</i>	MET proto-oncogene	141L	-6.53
MAPK14	α -Terpineol	<i>Homo sapiens</i>	Mitogen-activated protein kinase 14	1R3C	-6.53
NR3C1	(-)-Borneol	<i>Homo sapiens</i>	Nuclear receptor subfamily 3 group C member 1	3E7C	-6.48
NR3C1	(+)-Borneol	<i>Homo sapiens</i>	Nuclear receptor subfamily 3 group C member 1	3E7C	-6.48
ABL1	(-)-Borneol	<i>Homo sapiens</i>	ABL proto-oncogene 1	2F4J	-6.45
ABL1	(+)-Borneol	<i>Homo sapiens</i>	ABL proto-oncogene 1	2F4J	-6.45
MAP2K1	(-)- β -caryophyllene	<i>Homo sapiens</i>	Mitogen-activated protein kinase kinase 1	3EQC	-6.40

Table 4 continued. Molecular docking results of core targets and active components of ATR.

Gene	Composition	Specie	Protein	PDB ID	Estimated ΔG (kcal/mol)
MAP2K1	(+)- β -caryophyllene	<i>Homo sapiens</i>	Mitogen-activated protein kinase kinase 1	3EQC	-6.36
CASP3	(-)-Borneol	<i>Homo sapiens</i>	Caspase 3	2CJX	-6.34
PTPN1	α -Terpineol	<i>Homo sapiens</i>	Protein tyrosine phosphatase non-receptor type 1	1ONY	-6.32
MAP2K1	(+)-Borneol	<i>Homo sapiens</i>	Mitogen-activated protein kinase kinase 1	3EQC	-6.21

Table 5. Cell viability after 24-h incubation with various concentrations of $A\beta_{1-42}$.

Treatment	Neuronal survival (% CCK-8 reduction)
Control	100 \pm 4
DMSO alone	104 \pm 4 ^{ns}
25 μ mol/L $A\beta$ (1-42)	104 \pm 6 ^{ns}
50 μ mol/L $A\beta$ (1-42)	91 \pm 7 ^{a,#}
100 μ mol/L $A\beta$ (1-42)	76 \pm 7 ^{b,##}

ns – means no significant difference vs. control; ^b $P < 0.01$,
^a $P < 0.05$ vs. control; ^{##} $P < 0.01$, [#] $P < 0.05$ vs. DMSO alone.

database for component-related gene exploration and screened a total of 90 genes. Then, combined with AD-related genes screened by DisGeNET, 35 genes related to components and diseases were found, and the data were more accurate and reliable using these 2 databases. The network pharmacology approach is used to discover new therapeutic directions for drugs in natural products from the perspective of molecular biology networks. It provides a systematic means for pharmaceutically acceptable compounds in traditional Chinese medicines used in various complex diseases.

We successfully predicted the predictive targets of ATR, and the results of the PPI network suggested 13 hub genes. Among them, ESR1, PPARG, AR, CASP3, JAK2, MAPK14, MAP2K1, ABL1, PTPN1, NR3C1, MET, INSR, and PRKACA appear to play roles in treatment of AD by regulating various signaling pathways, including cancer pathways, MAPK signaling pathways, metabolic pathway, Ras signaling pathway, and PI3K-Akt signaling pathway.

Among the active components of ATR, β -asarone is one of the most popular research components. It has been found that it can improve the survival of neurons in APP/PS1 mice by reducing $A\beta$ deposition in the brain and downregulating $A\beta_{1-42}$

levels [21]. Cheng et al. found that oral β -caryophyllene can reduce the $A\beta$ load in the hippocampus and cerebral cortex and can prevent cognitive dysfunction in APP/PS1 mice [22]. Our docking results showed that β -caryophyllene has high docking stability with the target proteins. Therefore, we selected β -asarone and β -caryophyllene for qRT-PCR, showing that they can inhibit APP and Tau and regulate the mRNA levels of genes such as ABL1, ESR1, and JAK2. β -caryophyllene is an important component of ATR that can inhibit neuro-inflammation caused by $A\beta_{1-42}$ in BV-2 microglia [23]. Regarding the active ingredient gene of ATR, we explored the characteristics of its volatile oil components, which can improve AD by regulating hormone receptors such as ESR1, AR, NR3C1, and INSR. It affects the overexpression and degradation of $A\beta$ (e.g., PPARG and CASP3) and hyperphosphorylation of tau protein (e.g., MAPK14 and MAP2K1). It can also promote the growth and differentiation of nerve cells in the brain and inhibit apoptosis, thus promoting the growth of synapses. Differentiation (e.g., ABL1, MET, and PRKACA) reduces the intracerebral inflammatory response (e.g., JAK2 and PTPN1) to treat AD.

According to qPCR results, JAK2 and PTPN1 were significantly lower after being treated with the active ingredients. JAK2 and PTPN1 are associated with inflammatory responses. JAK2 participates in the non-receptor JAK2/STAT3 signaling pathway and is an important part of the neuroimmune response [23]. In addition, studies have found that downregulation of the PTPN1 gene can reproduce the AD-like phenotype in mice [24], and increasing the expression of PTPN1 can reduce the inflammatory response of microglia activated by STAT3 phosphorylation [25]. The related inflammation signaling pathway needs further research.

In summary, the anti-AD mechanism of ATR may be related to 13 genes, including ESR1, PPARG, AR, CASP3, and JAK2. This study preliminarily established a network model of the "disease-ingredient-target-pathway" of ATR in the occurrence of AD, and initially revealed the mechanism of the effect of the traditional Chinese medicine ATR.

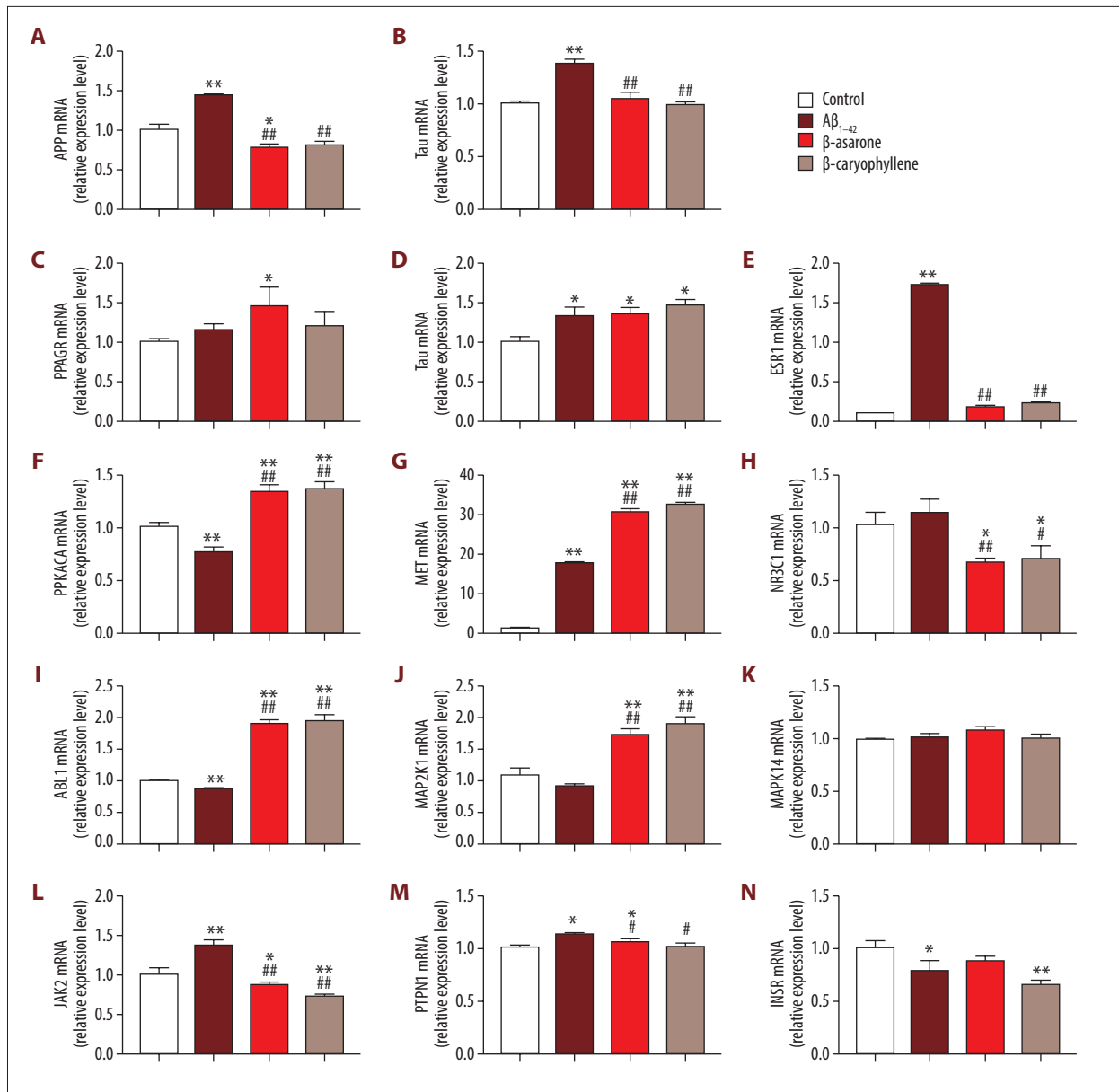


Figure 6. Cell experiments verified the docking results. (A, B) Relative expression level of APP and Tau mRNA; (C–N) Relative expression level of candidate gene mRNA. ** $4P < 0.01$; * $P < 0.05$ vs. control; ## $P < 0.01$; # $P < 0.05$ vs. Aβ₁₋₄₂ alone.

Conclusions

These findings suggest that ATR ameliorates neuronal damage caused by Aβ₁₋₄₂. ESR1, PRKACA, JAK2, PTPN1, and INSR were identified as therapeutic targets for further study of ATR to treat AD.

Acknowledgements

Thank Dr. Changyu Li and Dr. Liting Ji for helpful comments on the manuscript.

Availability of data and materials

The data used to support the findings of this study are available from the corresponding author upon request.

Ethics approval and consent to participate

All experimental protocols described in the present study were approved by Zhejiang Chinese Medical University.

Conflict of interests

None.

References:

- Ballard C, Gauthier S, Corbett A et al: Alzheimer's disease. *Lancet*, 2011; 377(9770): 1019–31
- Alzheimer's Association: 2016 Alzheimer's disease facts and figures. *Alzheimers Dementia*, 2016; 12(4): 459–509
- Zhu M, Tao Y, He Q et al: A common GSAP promoter variant contributes to Alzheimer's disease liability. *Neurobiol Aging*, 2014; 35(11): 2656.e1–e7
- The behavioural pharmacology of dementia. *Behav Pharmacol*, 2017; 28(2 and 3-Spec Issue): 91–93
- Mao J, Huang S, Liu S et al: A herbal medicine for Alzheimer's disease and its active constituents promote neural progenitor proliferation. *Aging Cell*, 2015; 14(5): 784–96
- He Q, Liu J, Lan JS et al: Coumarin-dithiocarbamate hybrids as novel multi-target AChE and MAO-B inhibitors against Alzheimer's disease: Design, synthesis and biological evaluation. *Bioorg Chem*, 2018; 81: 512–28
- Ambasta RK, Gupta R, Kumar D et al: Can luteolin be a therapeutic molecule for both colon cancer and diabetes? *Brief Funct Genomics*, 2018; 18(4): 230–39
- Xue J, Shi Y, Li C, Song H: Network pharmacology-based prediction of the active ingredients, potential targets, and signaling pathways in compound Lian-Ge granules for treatment of diabetes. *J Cell Biochem*, 2019; 120(4): 6431–40
- Liu AL, Du GH: [Network pharmacology: New guidelines for drug discovery.] *Yao Xue Xue Bao*, 2010; 45(12): 1472–77 [in Chinese]
- Li J, Lu C, Jiang M et al: Traditional chinese medicine-based network pharmacology could lead to new multicomponent drug discovery evidence-based complementary and alternative medicine. *Evid Based Complement Alternat Med*, 2012; 2012: 149762
- Ru J, Li P, Wang J et al: TCMSP: A database of systems pharmacology for drug discovery from herbal medicines. *J Cheminform*, 2014; 6: 13
- Wang X, Shen Y, Wang S et al: PharmMapper 2017 update: A web server for potential drug target identification with a comprehensive target pharmacophore database. *Nucleic Acids Res*, 2017; 45(W1): W356–60
- UniProt: A worldwide hub of protein knowledge. *Nucleic Acids Res*, 2019; 47(D1): D506–15
- Pinero J, Bravo A, Queralt-Rosinach N et al: DisGeNET: A comprehensive platform integrating information on human disease-associated genes and variants. *Nucleic Acids Res*, 2017; 45(D1): D833–39
- Szklarczyk D, Gable AL, Lyon D et al: STRING v11: Protein-protein association networks with increased coverage, supporting functional discovery in genome-wide experimental datasets. *Nucleic Acids Res*, 2019; 47(D1): D607–13
- Huang da W, Sherman BT, Lempicki RA: Bioinformatics enrichment tools: Paths toward the comprehensive functional analysis of large gene lists. *Nucleic Acids Res*, 2009; 37(1): 1–13
- Grosdidier A, Zoete V, Michielin O: Fast docking using the CHARMM force field with EADock DSS. *J Comput Chem*, 2011; 32(10): 2149–59
- Grosdidier A, Zoete V, Michielin O: SwissDock, a protein-small molecule docking web service based on EADock DSS. *Nucleic Acids Res*, 2011; 39(Web Server issue): W270–77
- Saleem F, Mehmood R, Mehar S et al: Bioassay directed isolation, biological evaluation and in silico studies of new isolates from *Pteris cretica* L. *Antioxidants (Basel)*, 2019; 8(7): pii: E231
- Zhang JY, Hong CL, Chen HS et al: Target identification of active constituents of Shen Qi Wan to treat kidney yang deficiency using computational target fishing and network pharmacology. *Front Pharmacol*, 2019; 10: 650
- Yang C, Li X, Mo Y et al: beta-Asarone mitigates amyloidosis and downregulates RAGE in a transgenic mouse model of Alzheimer's disease. *Cell and Mol Neurobiol*, 2016; 36(1): 121–30
- Cheng Y, Dong Z, Liu S: beta-Caryophyllene ameliorates the Alzheimer-like phenotype in APP/PS1 Mice through CB2 receptor activation and the PPARgamma pathway. *Pharmacology*, 2014; 94(1–2): 1–12
- Hu Y, Zeng Z, Wang B, Guo S: Trans-caryophyllene inhibits amyloid beta (Aβeta) oligomer-induced neuroinflammation in BV-2 microglial cells. *Int immunopharmacol*, 2017; 51: 91–98
- Wang ZH, Xiang J, Liu X et al: Deficiency in BDNF/TrkB neurotrophic activity stimulates delta-secretase by upregulating C/EBPbeta in Alzheimer's disease. *Cell Rep*, 2019; 28(3): 655–69.e5
- Wang X, Liu D, Huang HZ et al: A novel microRNA-124/PTPN1 signal pathway mediates synaptic and memory deficits in Alzheimer's disease. *Biol Psychiatry*, 2018; 83(5): 395–405
- Tsunekawa T, Banno R, Mizoguchi A et al: Deficiency of PTP1B attenuates hypothalamic inflammation via activation of the JAK2-STAT3 pathway in microglia. *EBioMedicine*, 2017; 16: 172–83